UNDERSEA & HYPERBARIC MEDICINE

In-field use of I-VED electrical impedance sensor for assessing post-dive decompression stress in humans

Sotiris P. Evgenidis, PhD[1]; Konstantinos Zacharias, PhD [1,2]; Virginie Papadopoulou, PhD [3,4,5]; Sigrid Theunissen, PhD[4]; Costantino Balestra, PhD[4]; Thodoris D. Karapantsios, PhD[1]

[1] Department of Chemical Technology and Industrial Chemistry, Faculty of Chemistry, Aristotle University, University Box 116, 541 24 Thessaloniki, Greece
[2] Physical Measurements Department, Hellenic Institute of Metrology, National Quality Infrastructure System, Block 45, 57022, Sindos, Thessaloniki, Greece
[3] Department of Bioengineering, Imperial College of London, London, UK
[4] Environmental & Occupational (Integrative) Physiology Laboratory, Haute Ecole Bruxelles-Brabant (HE2B), Brussels, Belgium
[5] Joint Department of Biomedical Engineering, The University of North Carolina at Chapel Hill and North Carolina State University, NC, USA

CORRESPONDING AUTHOR: Sotiris Evgenidis – sevgenid@chem.auth.gr

ABSTRACT

Evgenidis SP, Zacharias K, Papadopoulou V, Theunissen S, Balestra C, Karapantsios T. In-field use of I-VED electrical impedance sensor for assessing post-dive decompression stress in humans. Undersea Hyperb Med. 2024 First Quarter; 51(1):71-83.

Purpose: Ultrasound imaging is commonly used in decompression research to assess venous gas emboli (VGE) post-dive, with higher loads associated with increased decompression sickness risk. This work examines, for the first time in humans, the performance of a novel electrical impedance spectroscopy technology (I-VED), on possible detection of post-dive bubbles presence and arterial endothelial dysfunction that may be used as markers of decompression stress.

Methods: I-VED signals were recorded in scuba divers who performed standardized pool dives before and at set time points after their dives at 35-minute intervals for about two hours. Two distinct frequency components of the obtained signals, Low-Pass Frequency-LPF: 0-0.5 Hz and Band-Pass Frequency-BPF: 0.5-10 Hz, are extracted and respectively compared to VGE presence and known flow-mediated dilation trends for the same dive profile for endothelial dysfunction.

Results: Subjects with VGE counts above the median for all subjects were found to have an elevated average LPF compared to subjects with lower VGE counts, although this was not statistically significant ($p=0.06$), as well as significantly decreased BPF standard deviation post-dive compared to pre-dive ($p=0.008$).

Conclusions: I-VED was used for the first time in humans and operated to provide qualitative in-vivo electrical impedance measurements that may contribute to the assessment of decompression stress. Compared to ultrasound imaging, the proposed method is less expensive, not operator-dependent and compatible with continuous monitoring and application of multiple probes. This study provided preliminary insights; further calibration and validation are necessary to determine I-VED sensitivity and specificity.

Keywords: bubbles; decompression sickness; echocardiography; electrical impedance; endothelium; venous gas embolism

INTRODUCTION

Decompression sickness (DCS) is a pathophysiology resulting from ambient pressure decrease (decompression) in scuba divers, astronauts, and compressed air workers due to the formation and growth of bubbles in tissues as these equilibrate to the new reduced pressure [1]. Decompression bubbles may have mechanical effects (direct blood flow obstruction, impinging on nerve endings and thus causing pain and tissue tearing) or blood-bubble interfacial effects since they appear as foreign bodies in the organism and initiate a defense mechanism that triggers a cascade of reactions: vasoconstriction, leakage of liquids from the intravascular to extravascular spaces, platelets aggregation causing ischemia, blood viscosity increase, capillary flow resistance increase, capillary pressure increase, venous return decrease and blood flow decrease [2]. Symptoms vary, including musculoskeletal pain, mild cutaneous symptoms, neurological and cardiopulmonary manifestations [1]. Both external and individual factors influence the severity of DCS symptoms. External factors include the pressure profile the human body is subjected to (pressure difference, length of exposure, and decompression rate), the composition of the gas breathed in, the body movement during decompression, and the repetition of decompression exposures.

Furthermore, individual factors make subjects exposed to the same conditions before and during decompression react differently regarding DCS. The susceptibility to DCS seems to increase with age, body fat, previous DCS occurrence, and injury [2]. First-aid treatment for DCS includes administration of 100% oxygen, while definitive treatment refers to recompression to an increased pressure; adjunctive treatment, including fluid administration, is also recommended [3].

Circulating decompression bubbles in blood can often be detected post-dive, even after shallow asymptomatic dives, using ultrasound: either as audio signal shifts on precordial or subclavian Doppler, or as bright spots circulating in the venous chambers of the heart on B-mode echocardiography images [4-6]. Under normal conditions, these venous gas emboli (VGE) are effectively filtered by the lungs that trap and dissolve them so that they do not appear in the arterial circulation in the absence of paradoxical arterio-venous shunts such as Patent Foramen Ovale (PFO) [7]. VGE on echocardiography (or Doppler) is assessed by trained raters that assign a severity grade to the recording depending on the number of emboli present and their frequency of appearance over some cardiac cycles, following standardized classification. Higher VGE grades are statistically correlated with a higher probability of DCS [8,9], although asymptomatic divers with high grades are not uncommon. A new trend recently raised to consider, together with the classical VGE, some other "bubbles" that are inflammation-mediated cellular vesicles (microparticles) that could also contain gas and be fed by the surrounding inert gas supersaturation [10-12]. These decompression-related cellular responses may not be detectable by echocardiography [10]. Ultrasound imaging also quantifies Flow-Mediated Dilation (FMD) as a marker of the transient arterial endothelial dysfunction observed post-dive [13-15]. VGE and FMD ultrasonic measurements are highly operator-dependent in acquisition and interpretation [16,17], and clinical systems are incompatible with a wearable, low-cost, continuous imaging approach [18-20]. This is a major limitation, especially for data collection with limited space, time, and clinical personnel available and where the size of even portable clinical ultrasound scanners remains an operational challenge.

Bio-impedance sensors have been used as non-invasive medical diagnostics for over 40 years. Their applications range from respiratory plethysmography to cardiac stroke volume measurement and detection of bladder cancer [21]. Impedance changes in the content of the examined tissue provide information about the physiology and pathology of tissue and hemodynamic phenomena. Electrical bio-impedance depends on (i) the tissue and subject under study, (ii) the physiological and physicochemical variations within the tissues, (iii) the variation between healthy and unhealthy tissues, and (iv) the frequency of applied signal [22]. Bio-impedance sensors may overcome the aforementioned limitations of ultrasound imaging since they do not need special training and experience to operate, and their

compatibility with (inexpensive) wearable technology is already mature. Additionally, multiple and continuous impedance measurements are feasible by applying electrodes of the right size, shape, and geometry [23,24].

An electrical impedance spectroscopy technique called I-VED (EU patent: EP 3 005 942 A1, 2016) was developed for non-invasive, real-time bubbles detection in humans, under the umbrella of the European Space Agency Project *"In-Vivo Embolic Detector, I-VED"* (Contract No.: 4000101764, 2004-2014). I-VED was previously calibrated and validated in-vitro, using a benchtop flow-loop that provided well-controlled bubbly flow with liquid velocities, bubble sizes, and gas volumetric concentrations similar to those observed during DCS, and its sensitivity was found two orders of magnitude higher than conventional electrical techniques [25-30]. This study aims to examine I-VED performance on decompression stress quantification in humans for the first time. For this, pre and post-dive electrical impedance signals in scuba divers that perform well-controlled pool dives are compared to echocardiography for VGE presence, and to FMD trends for the same dive profile in prior work.

METHODS

Study population, dive profile and measurement timings

All experiments were conducted in accordance with the Declaration of Helsinki (World Medical Association, 2013) after approval by the Academic Ethical Committee of Brussels and volunteer informed consent. Seventeen healthy, non-smoker male volunteer divers (42 ± 7 years old, BMI = 25.2 ± 1.9 kg.m^{-2}) were recruited from a larger cohort of sport divers to dive over two days in the evening, either once or twice (24 hours apart). Selection criteria included certification to the level of 'autonomous diver' or above (EN 14153-2 or ISO 24801-2), a minimum of 50 logged dives, a 'fit to dive' medical clearance, no history of DCS, not on cardio-active medications.

Divers dived in pairs: on the first day five pairs were measured (n=10 subjects), and on the second day four pairs dove (n=7 subjects because one of the buddy pairs acted as a diving buddy only). The dive consisted of the standardized pool environment (NEMO 33, Brussels, Belgium) profile that has been used extensively in prior literature: 20 minutes to a depth of 33 meters fresh water (mfw) (400 kPa), e.g. [14,31,32]. Three measurement stations were organized so that each volunteer buddy pair rotated between all stations at controlled time intervals (every 35 minutes, they would be measured at the same station), starting at 14 minutes post water exit. Each station, therefore, had a baseline pre-dive measurement and four measurements post-dive at 35 minutes intervals. The first station consisted of some basic anthropomorphic measurements (weight, height, impedance balance, and urine-specific gravity as a hydration indication), and other measurements are described hereafter. To isolate the effect of bubble presence and endothelial dysfunction on the acquired I-VED signals, divers were instructed to restrict fluid intake post-dive for the study to minimize changes in skin hydration, which can confound measurements.

Standard decompression stress assessment: echocardiography measurements

Volunteers were positioned on a mat, lying on their left side with their left arm under their head for support. VGE were detected using B-mode trans-thoracic echocardiography (TTE) with a sectorial cardiac transducer (SP5-1S) on a portable ultrasound scanner (M9, Mindray Bio-Medical Electronics Co, Shenzhen, China), in standard adult echocardiography mode (imaging frequency 3.4 MHz, 30 Hz frame rate, mechanical index MI=1.2). VGE load was assessed using a validated counting method [33]. At each measurement time-point, modified four-chamber view recordings comprising at least ten consecutive cardiac cycles are saved for later analysis. For analysis, the experimenter can scroll through the video frame by frame. For each cardiac cycle, bubbles are counted on a frame where the tricuspid valves are open (to minimize misclassifications). The 'bubble score' for each recording is taken as the average of ten consecutive cardiac cycle counts.

I-VED data acquisition and processing

The I-VED technique, as previously developed and validated in vitro [25-27,29,30], was utilized to read bio-impedance signals through a pair of ECG-type electrodes placed at the left forearm site of divers (Fig. 1a). Hereafter, the basic mode of I-VED operation in conjunction with the rationale for possible correlations to VGE and FMD is described. A sinusoidal current signal with a frequency of 70 KHz and amplitude of 0.5 mA RMS is applied through the two electrodes. Frequency scanning from 10 to 90 KHz showed that the excitation frequency of 70 KHz provides the lowest phase shift and the highest signal-to-noise ratio. Considering that most biomedical devices operate with stimulation currents of a few mA, an excitation current amplitude of 0.5 mA RMS was considered adequate for this study. The current source excitation is accomplished by employing a custom-made, alternating current Voltage Controlled Current Source (VCCS). The magnitude of VCCS transfer function ($|H_{VCCS}|$) was adjusted as follows:

$$|H_{VCCS}| = \frac{0.5\text{mA}}{0.5\text{V}} = 0.001$$

Input voltage of 0.5 V is transformed (converted) to output excitation current (I_{out}) of 0.5 mA passing through the electrode E1. The VCCS is located between the voltage source and the electrode E1, Fig. 1b (*i*). Fig. 1b (*ii*) shows the corresponding electrical equivalent of the measurement set-up. V_g is the output voltage of the signal generator, $V_m = V_{E1}\text{-}V_{E2}$ is the differential voltage measured across the electrodes E1 and E2 caused by the excitation current of the VCCS, Z_m is the measured impedance between the two applied electrodes, and R_{cm} is an optional resistor for current sensing.

The measured impedance as "sensed" by the electrodes E1 and E2 is the magnitude of Z_m, which is calculated as follows:

$$Z_m = \frac{V_{E1}\text{-}V_{E2}}{I_{out}} = \frac{V_m}{I_{out}}$$

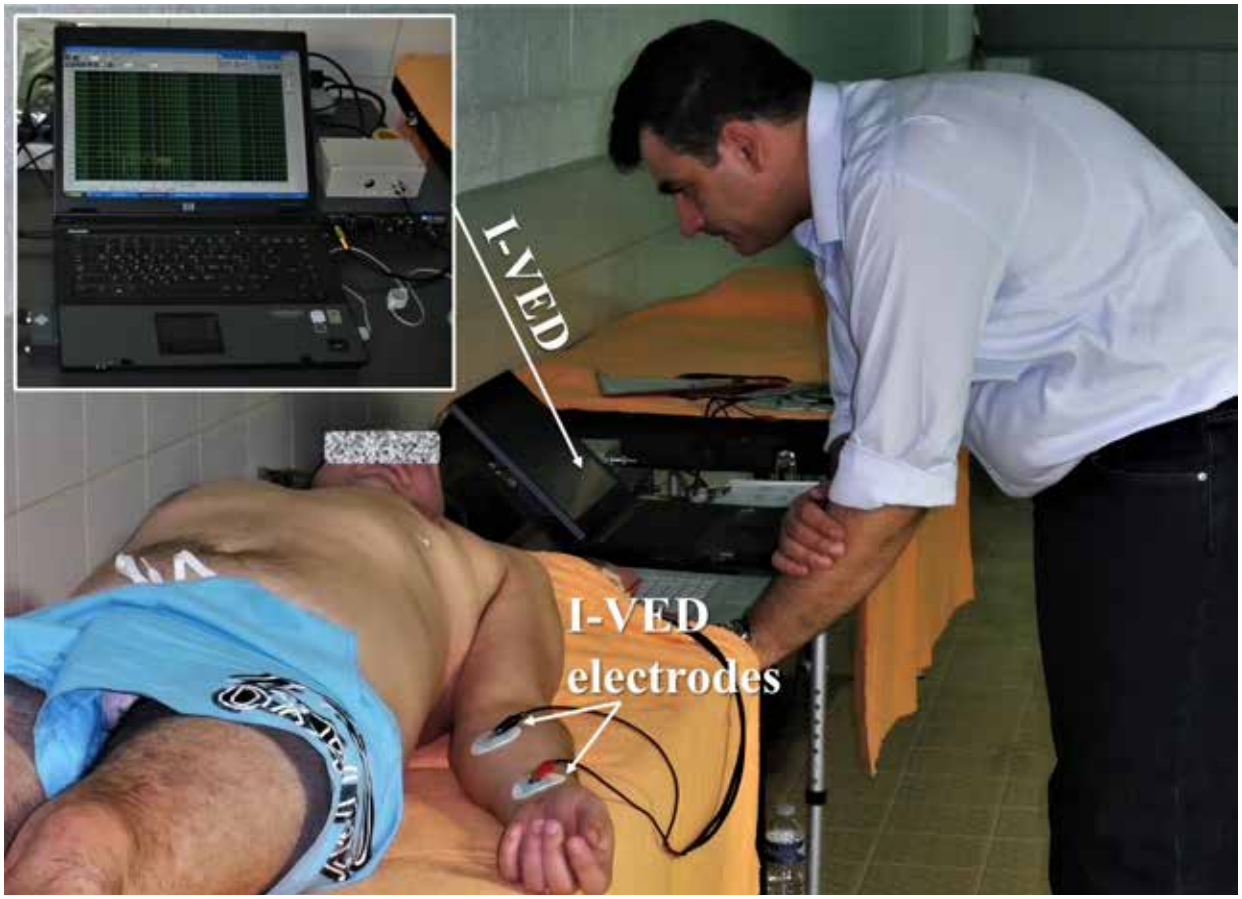

Figure 1a. Execution of I-VED measurement

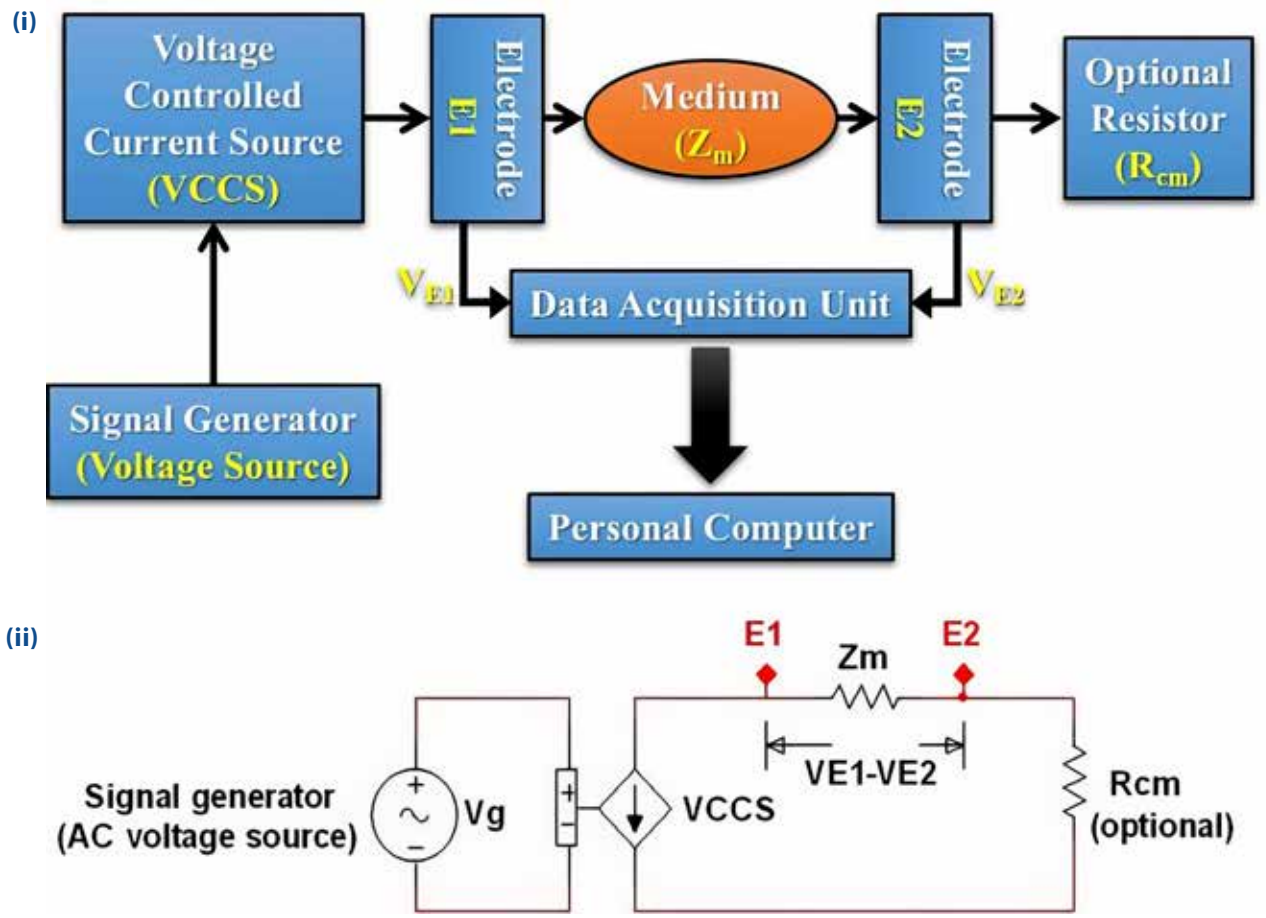

Figure 1b. **(i) Design logic (ii) Electrical equivalent of I-VED electrical impedance technique applying current source excitation mode.**

The voltage difference V_m is the measured key parameter (I_{out} is constant) because it is directly affected by impedance variation due to the presence of bubbles and/or endothelial dysfunction. V_m is recorded by a high-resolution (24-bit) data acquisition card (E-MU 1616m, CREATIVE Professional) with a sampling frequency of 192 kHz, that allows to: a) investigate electrical signals of frequency up to 96 kHz and b) measure extremely low voltages down to a few microvolts. Then, the recorded AC signals of V_m are digitally processed by custom-made software that complements I-VED hardware. First, a band pass filter centered at 70 kHz with 3 kHz bandwidth is applied to reject all kinds of electrical interference. The envelope of filtered AC signals is then digitally extracted taking the absolute value in Matlab. This non-linear process creates high-frequency artifacts, which are removed by a low-pass filter (nominal cut-off frequency of 100 Hz). So far, conventional electrical techniques using analog electronics do not have filters for electrical interference rejection, or these filters are not effective and selective enough. Consequently, measurement accuracy and sensitivity have substantially deteriorated [34-36].

I-VED captures voltage differences lower than 1μV corresponding to resistance variation, ΔR/R, of 0.001%. According to the specifications of the data acquisition card, the maximum measured voltage is V_{max}= 1.2277 V_{RMS}. The peak-to-peak voltage of V_{max} is equal to the Full Scale voltage (VFS) of the Analog-to-Digital Converter (ADC) of the data acquisition card; therefore $V_{FS} = V_{maxp\text{-}p}$ = 3.4723 V. The resolution of the ADC is n=24 bits, so the quantization voltage V_{LSB}, which represents the minimum voltage difference that the ADC can measure and convert, is $V_{LSB} = V_{FS}/2^n$ = 0.2 μV. On the other hand, classical electrical methods could not sense voltage differences lower than 1mV [34-36]. The so-filtered enve-

lope of V_m signals constitutes the real peak voltage amplitude of acquired signals without any loss of information or distortion and is utilized for Z_m calculation. The final output of signal processing is several 30 second-long Z_m time-series for different divers and time points.

Z_m time-series analysis in frequency domain shows that full spectrum ranges from 0 Hz to 100 Hz, which can be decomposed into three critical frequency band components [37]: a) LPF: Low-Pass Frequency component from 0 Hz to 0.5 Hz associated with mean impedance value of blood (applying an acausal 8th order low-pass filter with cut-off frequency at 0.5 Hz), b) BPF: Band-Pass Frequency (cardiac) component from 0.5 Hz to 10 Hz, associated with heartbeats (applying an acausal 8th order band-pass filter with low cut-off frequency at 0.5 Hz and high cut-off frequency at 10 Hz), c) HPF: High-Pass Frequency component from 10 Hz to 100 Hz associated with cardiac component harmonics and measurement noise (applying an acausal 8th order high pass filter with cut-off frequency at 10 Hz).

A representative raw electrical impedance signal as a function of time is shown in Fig. 2, together with the three extracted frequency component time series (LPF, BPF, HPF). Although the acquired and processed impedance signals last 30 sec, Figs. 2a, 2b, 2c, and 2d display electrical impedance only for ten seconds to discern typical signal features such as the intensity and frequency of observed fluctuations.

The raw signal (0-100 Hz) displays a repeatable pattern every ~1 sec associated with the cardiac cycle (Fig. 2a). Impedance variation for each cardiac cycle is less than 100 mOhm. Additionally, much smaller and faster impedance changes superimposed over the slow ones around 1 Hz are also captured. The extracted LPF time-series (0-0.5 Hz, Fig. 2b) is associated with mean blood impedance value, which depends on blood flow velocity, blood volume, and orientation of blood cells. These quantities cannot fluctuate considerably for the recording time of 30 seconds. Thus, LPF signal demonstrates a relevant stability where impedance variation over 10 sec does not exceed 20 mOhm (Fig. 2b). The pattern associated with the cardiac cycle is shown more clearly in the extracted BPF time-series (0.5-10 Hz, Fig. 2c). In each cardiac cycle that lasts ~1 sec (corresponding to 60 heartbeats), three phases can be noticed: a) a rapid and large increase of impedance (25±5 mOhm in ~0.1 sec), b) a small additional, and slower, impedance increase (15±5 mOhm in ~0.8 sec) and c) a rapid decrease of the impedance down to the initial value (~40 mOhm in ~0.1 sec). The HPF time series (10-100 Hz, Fig. 2d) is characterized by very fast impedance fluctuations of around 20 mOhm. However, such high frequencies cannot be correlated with parameters of human physiology and, therefore, are considered as "electrical" noise.

Based on the above, we hypothesized that: a) LPF impedance will increase with post-dive VGE presence since the electrical resistivity of gas bubbles is several orders of magnitude higher compared to blood (electrically conductive medium), so VGE presence is expected to increase its mean impedance value; and b) BPF impedance variation will decrease post-dive

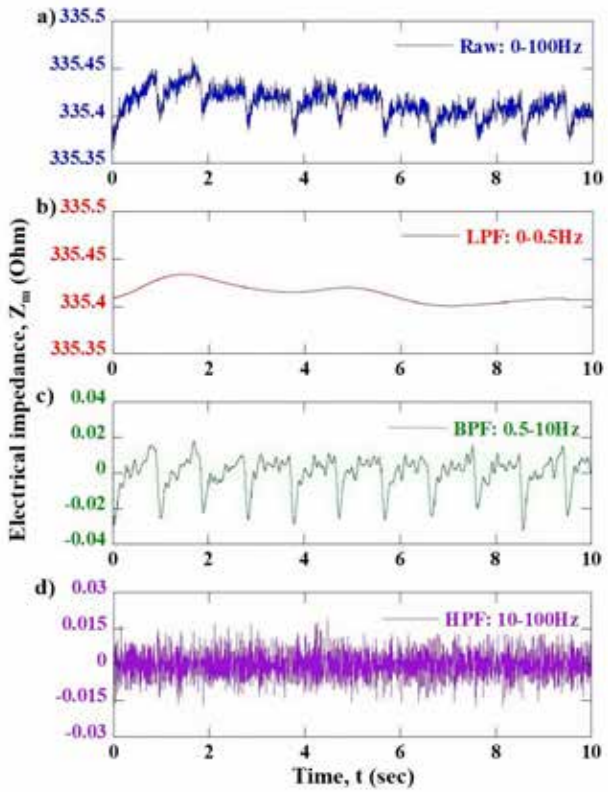

Figure 2. **(a) Representative example of raw electrical impedance signal as a function of time (b) Extracted Low-Pass Frequency component time-series (LPF: 0-0.5 Hz) (c) Extracted Band-Pass Frequency component time-series (BPF: 0.5-10 Hz) (d) Extracted High-Pass Frequency component time-series (HPF: 10-100 Hz).**

during transient endothelial dysfunction due to the attenuation of blood flow fluctuations as a result of increased arterial stiffness [38].

Statistical analyses

The I-VED metrics of $LPF_{average}$ (average impedance value for each 30 sec-long LPF time-series) and BPF_{stdev} (standard deviation of impedance for each 30 sec-long BPF time-series) were investigated with respect to post-dive bubbles presence and endothelial dysfunction, respectively. To quantify the variability of each metric at a specific time-point, the Coefficient of Variation (CV, %) was calculated as follows: *CV = ((standard deviation of metric)/(mean value of metric))* x 100. Statistical analysis was performed in GraphPad Prism version 5.01 (GraphPad Software, San Diego, California, USA). Data are presented as mean ± standard deviation and statistical significance is set a priori at $p<0.05$ and denoted graphically as * for $p<0.05$ and ns for $p>0.05$. Since this study constitutes the first-in-human pilot study with I-VED, pilot data were also used to calculate the sample sizes needed for future work [39,40].

A two-tailed Mann-Whitney-Wilcoxon test after the negative normality test (D'Agostino and Pearson omnibus normality test) was used to assess whether LPF values for all measurement time points were higher for higher VGE counts compared to the lower VGE counts on echocardiography. The echocardiography threshold between low and high bubblers was defined as the bubble count median value for this dive profile, equal to 4.3 (in other words, separating the 50% higher and 50% lower bubbling subjects at the first measurement time point post-dive, which is highest in terms of VGE). In addition, the ability of the $LPF_{average}$ metric to serve as a classifier between low and high bubblers was assessed by building a receiver-operator characteristic (ROC) curve. This ROC plots the true positive rate (sensitivity) against the true negative rate (1 – specificity) as the classifier threshold varies. Performance was assessed by the area under the curve (AUC) reported with its 95% confidence interval (CI) denoted as CI: lower bound – upper bound, where a theoretically perfect classifier would correspond to an AUC of 1, and random classification by chance to 0.5.

FMD decreases around 30-60 minutes after a dive profile such as the one performed in the present study due to transient endothelial dysfunction that limits vasodilation [14]. If BPF_{stdev} metric is correlated to FMD, we expect it to decrease post-dive and eventually recover pre-dive values. This was tested by comparing the BPF_{stdev} evolution post-dive with the respective pre-dive values, using a Friedman test with Dunn's post-test for multiple comparisons to baseline after the negative normality test (D'Agostino and Pearson omnibus normality test). Also, the standard deviations of BPF_{stdev} values at each post-dive time-point were compared to the pre-dive ones using the F-test, as implemented in MedCalc® Statistical Software version 20.110 (MedCalc Software Ltd, Ostend, Belgium). P-values after Bonferroni correction for multiple-tests are reported.

RESULTS

The $LPF_{average}$ metric was not able to distinguish between VGE = 0 and VGE > 0 (data not shown). Instead, we noticed a trend for $LPF_{average}$ to increase in time points with higher VGE counts (VGE > 4.3, n = 19 time points) compared to those with lower VGE counts (VGE ≤ 4.3, n = 49 time points) (Fig. 3a), although this variation fails to reach statistical significance ($p = 0.06$). The ROC analysis resulted in an AUC of 0.64 [CI: 0.49 – 0.79] with $p = 0.06$ (Fig. 3b). When focusing on the evolution of $LPF_{average}$ post-dive compared to pre-dive for the diving group (n = 17), there is an indication that $LPF_{average}$ variation may increase temporarily in the first post-dive measurement and then decreases and remains almost constant from the second to the fourth post-dive measurement (Fig. 4a). However, this change of $LPF_{average}$ variation was not shown to be statistically significant.

The BPF_{stdev} metric was hypothesized to diminish post-dive due to reduced vasodilation caused by transient endothelial dysfunction. Although the average value of BPF metric for the diving group (n = 17) practically decreases post-dive compared to pre-dive, no relevant statistical difference was found. Instead, the standard deviation of the abovementioned metric around its average, demonstrating the dispersion of measurements for the diving group at a certain time-point, was statistically significantly

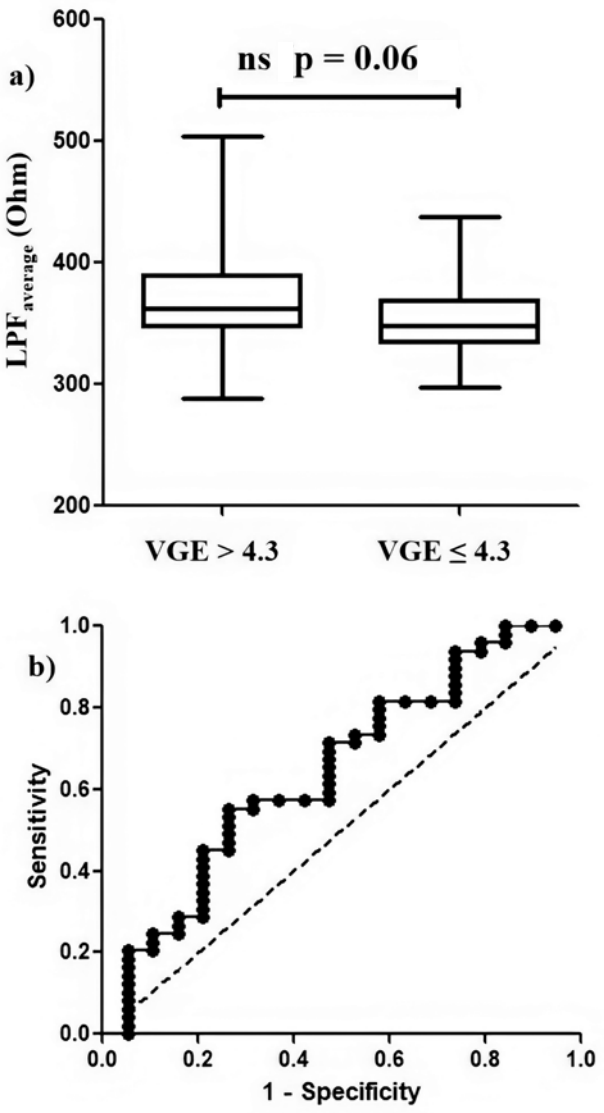

Figure 3. (a) Comparison of $LPF_{average}$ values for high bubblers (VGE > 4.3, n = 19 time points) and low bubblers (VGE ≤ 4.3, n = 49 time points) (b) ROC analysis to assess the performance of $LPF_{average}$ metric as a classifier between low and high bubblers.

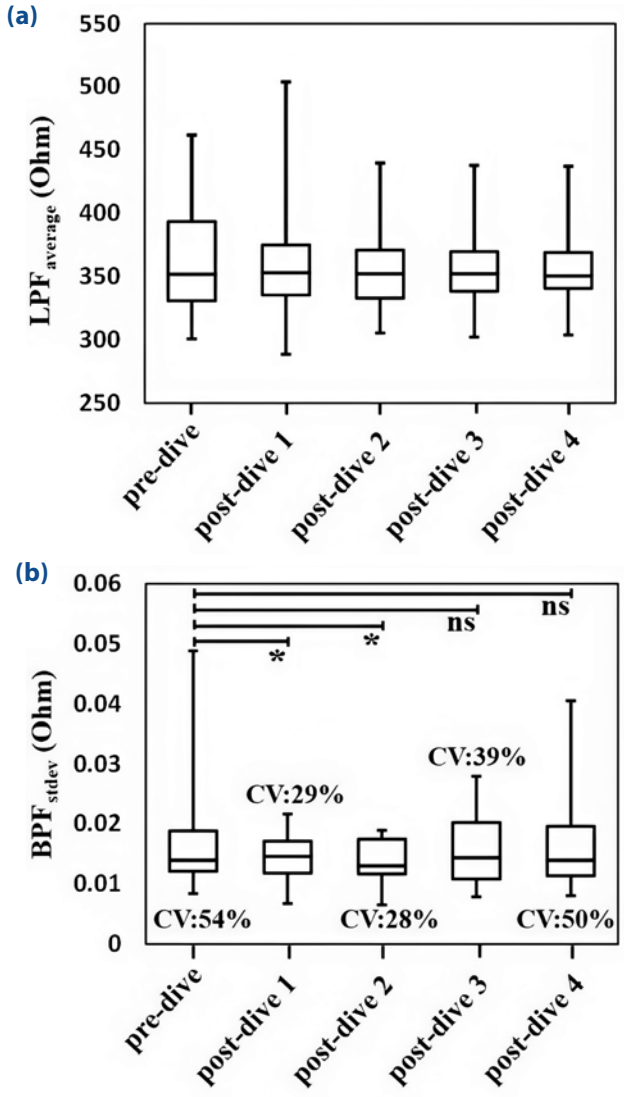

Figure 4. Evolution of a) $LPF_{average}$ metric (b) BPF_{stdev} metric post-dive compared to pre-dive (n = 17). Post-dive 1: 28 min post-dive, post-dive 2: 63 min post-dive (post-dive 1 + 35 min), post-dive 3: 98 min post-dive (post-dive 2 + 35 min), post-dive 4: 133 min post-dive (post-dive 3 + 35 min).

decreased post-dive as a response to the temporary impaired endothelium-dependent vasodilation that makes BPF signals fluctuating less (Fig. 4b). Specifically, BPF_{stdev} metric variability was high before the dive (Coefficient of Variation, CV: 54%), lowered considerably at the first two post-dive measurements (CV: 29% and CV: 28%, respectively), started to increase at the third post-dive measurement (CV: 39%) and almost reached the pre-dive state at the fourth post-dive measurement (CV: 50%). Statistical analysis showed that the BPF_{stdev} metric standard deviations of both post-dive 1 and post-dive two time-points were significantly different from the pre-dive one (p=0.008 and p=0.004, respectively), while no significant differences were found for post-dive three and post-dive four time-points. Moreover, the distribution of BPF_{stdev} values before and 120 minutes after the dive showed a divergence - by a qualitative point of view - from the normal distribution (positively skewed and platykurtic with positive kurtosis).

DISCUSSION

In this first-in-human pilot study, the I-VED electrical impedance method was used for possible detection of the presence of post-dive bubbles and arterial endothelial dysfunction. From a technical point of view, we performed the electrical measurements without problems with electrode positioning at the forearm, electrical lead connections, acquisition and storage of signals. Provided this technique can yield useful information, I-VED may be an attractive and easy-to-use platform for possible decompression stress evaluation.

The LPF frequency component (0-0.5 Hz) of the acquired signals, related to mean blood impedance value, was exploited as a possible indicator for VGE presence. Based on our hypothesis, the $LPF_{average}$ metric was not higher for VGE > 0. However, it was shown to be higher for VGE > 4.3, although this variation was not statistically significant ($p = 0.06$). At least 44 subjects in each group would be needed to confirm a two-tailed statistical difference between medians with 80% power and an alpha p-value of 0.05 [39,40]. Considering the actual understanding of decompression stress and the fact that some of the decompression-related responses in terms of circulating gas containing microparticles or tissue micronuclei may not be detectable by echocardiography [10], it is concluded that: a) I-VED calibration against echocardiography may be practically inadequate and b) I-VED may be a promising system to tackle this specific side of decompression since its measuring sensitivity may be high enough to sense the presence of such gas containing microparticles or tissues. The observed increase in LPF signal variation in the first post-dive measurement could be related to the re-positioning of electrodes before the first post-dive measurement combined with varying skin hydration of divers a few minutes after their exit from the water. This may explain why the normalized post-dive $LPF_{average}$ data concerning the pre-dive value do not provide any remarkable outcome concerning the correlation with VGE count and, consequently, the reason that raw post-dive $LPF_{average}$ data are exploited here instead. In any case, non-conclusive results on bubble numbers assessed by echocardiography, and the coefficient of variation increase at compatible time points related to gas microparticles or tissue micronuclei increase post-exposure [10] are of great interest.

BPF frequency component (0.5-10 Hz) of obtained I-VED signals, associated with heartbeats, was examined as an indicator for post-dive endothelial dysfunction using BPF_{stdev} metric. Although the mean value of BPF metric for the diving group did not show any remarkable change, its standard deviation showed a statistically significant decrease temporarily post-dive, which is also associated with the transient endothelial dysfunction as explained below: During post-dive endothelial dysfunction period, endothelium-dependent vasodilation impairs and, as a result, blood flow fluctuations attenuate. Therefore, BPF signal amplitude, and the estimated BPF_{stdev} value, shall be temporarily diminished post-dive. Although statistical analysis does not validate this change, it is noticed that the dispersion of measured BPF_{stdev} values, as expressed by the standard deviation of BPF metric around its average for the diving group (n=17) at a certain time-point, is significantly limited post-dive due to the less fluctuating signals. This constitutes a first, still valuable indication of I-VED BPF metric correlation with endothelial functionality that may improve by improving the experiment design (e.g., including simultaneous FMD measurements).

Overall, I-VED provides stable bio-impedance signals free of electrical interference, including two distinct frequency bands known to correlate to blood impedance values and heartbeats [37]. Nevertheless, the I-VED method needs further development, accompanied with several calibration and validation tests to contribute substantially and reliably in the assessment of decompression stress. The design of future trials on humans should focus on: a) the synchronization of ultrasonography and impedance measurements to improve validation of obtained results, b) Collecting more data with the increase of study population and number of post-dive measurements, to enhance statistical analysis and c) the assessment of the interplay between I-VED metrics and other post-dive physiological changes such as hydration, oxidative stress and inflammation that may affect measured values.

Furthermore, in-vivo tests on animals or blood vessel phantoms performing well-controlled infusion of varying bubble sizes and quantities [41], could facilitate significantly I-VED calibration and validation under well-controlled conditions. The idea of determining I-VED sensitivity and specificity over binary DCS outcomes (based on symptoms) from animals could also be considered. Swines seem to be a wise option for I-VED in-vivo testing because their cardiovascular system is comparable with that of humans. Identifying the proper measurement points over the swines' skin, where the electrical properties of the intervening tissues effectively imitate those of humans, is considered a major challenge. Furthermore, although the population and size of bubbles to be infused in the swines' bloodstream will be well-defined, their behavior is questionable once they enter the bloodstream. Coalescence phenomena or/and attachment of bubbles to the vessel walls may occur and hamper I-VED calibration. However, applying simultaneous ultrasound measurements at the same location where I-VED measurements are conducted is expected to shed light on bubble behavior and, consequently, facilitate I-VED calibration.

LIMITATIONS

Several limitations were present in this first-in-human pilot study. Starting with subject recruitment, a limitation of the study is the restriction to male subjects. This was a practical limitation related to the sample size of our experiment, partly justified by the over-representation of male divers in the professional diving population of interest. It is, however, conceded that there is a large population of female recreational divers and a growing population of female divers in commercial and military settings. This may be significant given that the limited studies investigating sex-related differences in VGE support a hormonal cycle influence [42-44], though their implication regarding DCS susceptibility is unclear [45].

Most notably, there was no temporal or anatomical synchronization between echocardiography and I-VED measurements. I-VED was taken on average seven minutes after echocardiography, and it is possible that VGE will increase/decrease during this time. This temporal mismatch may cause severe disagreement between I-VED and echocardiography measurements for the entire range of VGE counts; however, this disagreement will be intensified for low but non-zero VGE counts (<1) where one VGE is not consistently observed on every cardiac cycle. Additionally, ultrasound measurements were recorded in the heart, whereas I-VED was positioned on the forearm and measured in a separate location. It is difficult to ascertain how this would influence quantification, and additional ultrasound measurements in the brachial region may be warranted in future studies.

Additionally, removing and repositioning the electrodes before the first post-dive measurement may confound the use of the pre-dive measurement to serve as a true baseline. Future studies will need to elucidate the effect of such repositioning with respect to other physiological changes associated with the dive (thermal, hydration, exercise, etc). Finally, a major limitation is the absence of simultaneous FMD measurements in this study, which does not allow for a direct correlation of the BPF_{stdev} metric with endothelial functionality.

CONCLUSIONS

In this pilot study, an electrical impedance spectroscopy technique (I-VED), originally developed for space applications, was used to measure scuba divers pre- and post-dive for the first time. Measurements were easy to acquire and provided ''stable" electrical signals. Distinct frequency components were not proven capable of detecting post-dive bubble presence and endothelial dysfunction. The difference in $LPF_{average}$ metric between low and high bubblers concerning this dive's median echocardiography bubble count was also not statistically significant. While this may partially be due to insufficient experimental design and power in this pilot study (a post-hoc power calculation determined that at least 44 subjects per group would be needed to determine this with 80% power and alpha p-value of 0.05), the lack of statistical significance should be handled with caution. Furthermore, the standard deviation of BPF_{stdev} was shown statistically different temporarily post-dive compared to pre-dive and this is a first, still valuable, indication of BPF metric

correlation with endothelial functionality. Future studies will focus on optimizing the design of in-vivo trials and investigating in depth the role of different physiological parameters on the obtained results to evolve I-VED technology and evaluate its performance for measuring decompression stress.

DECLARATIONS

Ethics Approval

This study was performed in line with the principles of the Declaration of Helsinki. Approval was granted by the Academic Ethical Committee of Brussels Alliance for Research and Higher Education (Date: 05-05-2014 / No: B200-2014-046)

Consent to participate

Informed consent was obtained from all individual participants included in the study.

Funding

This research was co-financed by Greece and the European Union (European Social Fund-ESF) through the Operational Programme «Human Resources Development, Education and Lifelong Learning» in the context of the project "Reinforcement of Postdoctoral Researchers" (MIS-5001552), implemented by the Greek State Scholarships Foundation (ΙΚΥ).

Conflict of interests

S.P.E., K.Z. and T.D.K. declare that they are co-inventors on I-VED patent developed for non-invasive, real-time bubbles detection in humans (EP 3 005 942 A1, 2016). V.P., S.T. and C.B. declare no competing interests.

Acknowledgements

The authors would like to thank all the volunteers who participated in this study, as well as the NEMO pool for allowing us to use their facilities.

REFERENCES

1. Mitchell SJ, Bennett MH, Moon, RE. Decompression Sickness and Arterial Gas Embolism. N. Engl. J. Med. 2022;386:1254-1264. doi: 10.1056/NEJMra2116554. PMID: 35353963.

2. Rudge FW, Zwart BP, Effects of decreased pressure: Decompression Sickess. Flight Surgeon Guide-Chapter 3 Hyperbarics 2002.

3. Jitsuiki K, Kushida Y, Nishio R, Yanagawa Y. Gas in joints after diving: Computed tomography may be useful for diagnosing Decompression Sickness. Wilderness Environ Med. 2021;32(1):70-73. doi: 10.1016/j.wem.2020.09.006.

4. Balestra C, Guerrero F, Theunissen S, Germonpre P, Lafere P. Physiology of repeated mixed gas 100-m wreck dives using a closed-circuit rebreather: a field bubble study. Eur. J. Appl. Physiol. 2022;122:515-22. doi: 10.1007/s00421-021-04856-5. PMID: 34839432. PMCID: PMC8627581.

5. Dugrenot E, Balestra C, Gouin E, L'Her E, Guerrero F. Physiological effects of mixed-gas deep sea dives using a closed-circuit rebreather: a field pilot study. Eur. J. Appl. Physiol. 2021;121:3323-31. doi: 10.1007/s00421-021-04798-y. PMID: 34435274.

6. Lambrechts K, Germonpre P, Vandenheede J, Delorme M, Lafere P, Balestra C. Mini Trampoline, a New and Promising Way of SCUBA Diving Preconditioning to Reduce Vascular Gas Emboli? Int. J. Environ. Res. Public Health 2022;19:5410. doi: 10.3390/ijerph19095410. PMID: 35564805. PMCID: PMC9105492.

7. Germonpre P, Lafere P, Portier W, Germonpre FL, Marroni A, Balestra C. Increased Risk of Decompression Sickness When Diving With a Right-to-Left Shunt: Results of a Prospective Single-Blinded Observational Study (The "Carotid Doppler" Study). Front. Physiol. 2021;12:763408. doi: 10.3389/fphys.2021.763408. PMID: 34777020. PMCID: PMC8586212.

8. Eftedal OS, Lydersen S, Brubakk AO. The relationship between venous gas bubbles and adverse effects of decompression after air dives. Undersea Hyperb. Med. 2007;34(2):99–105. PMID: 17520861.

9. Sawatzky KD. The relationship between intravascular Doppler detected gas bubbles and decompression sickness after bounce diving in humans. Toronto (CA), York University, 1991.

10. Arya AK, Balestra C, Bhopale VM, Tuominen LJ, Raisanen-Sokolowski A, Dugrenot E, L'Her E, Bhat AR, Thom SR. Elevations of Extracellular Vesicles and Inflammatory Biomarkers in Closed Circuit SCUBA Divers. Int. J. Mol. Sci. 2023;24:5969. doi: 10.3390/ijms24065969.

11. Balestra C, Germonpre P, Rocco M, Biancofiore G, Kot J. Diving physiopathology: the end of certainties? Food for thought. Minerva Anestesiol. 2019;85:1129-1137. doi: 10.23736/S0375-9393.19.13618-8. PMID: 31238641.

12. Balestra C, Arya AK, Leveque C, et al. Varying Oxygen Partial Pressure Elicits Blood-Borne Microparticles Expressing Different Cell-Specific Proteins-Toward a Targeted Use of Oxygen? Int. J. Mol. Sci. 2022;23:7888. doi: 10.3390/ijms23147888.

13. Brubakk AO, Duplancic D, Valic Z, Palada I, Obad A, Bakovic D, Wisloff U, Dujic Z. A single air dive reduces arterial endothelial function in man. J. Physiol. 2005;566(Pt 3):901–906. doi: 10.1113/jphysiol.2005.089862. PMID: 15961424. PMCID: PMC1464788.

14. Theunissen S, Guerrero F, Sponsiello N, Cialoni D, Pieri M, Germonpré P, Obeid G, Tillmans F, Papadopoulou V, Hemelryck W, Marroni A, De Bels D, Balestra C. Nitric oxide-related endothelial changes in breath-hold and scuba divers. Undersea Hyperb. Med. 2013;40(2):135-144. PMID: 23682545.

15. Zhang K, Wang D, Jiang Z, Ning X, Buzzacott P, Xu W. Endothelial dysfunction correlates with decompression bubbles in rats. Scientific Reports 2016;6:33390. doi: 10.1038/srep33390. PMID: 27615160. PMCID: PMC5018851.

16. Blogg SL, Gennser M. The need for optimisation of post-dive ultrasound monitoring to properly evaluate the evolution of venous gas emboli. Diving Hyperb. Med. 2011;41(3):139–146. PMID: 21948499.

17. Mollerlokken A, Blogg SL, Doolette DJ, Nishi RY, Pollock NW. Consensus guidelines for the use of ultrasound for diving research. Diving Hyperb. Med. 2016;46(1):26–32. PMID: 27044459.

18. Le DQ, Dayton PA, Tillmans F, Freiberger J, Moon R, Denoble P, Papadopoulou V. Ultrasound in Decompression Research: Fundamentals, Considerations, and Future Technologies. Undersea Hyperb. Med. 2021;48(1):59-72. PMID: 33648035.

19. Thijssen DHJ, Black MA, Pyke KE, Padilla J, Atkinson G, Harris RA, Parker B, Widlansky ME, Tschakovsky ME, Green DJ. Assessment of flow-mediated dilation in humans: a methodological and physiological guideline. Am. J. Physiol. Heart Circ. Physiol. 2011;300:2-11. doi: 10.1152/ajpheart.00471.2010. PMID: 20952670. PMCID: PMC3023245.

20. Thijssen DHJ, Bruno RM, van Mil ACCM, Holder SM, Faita F, Greyling A, Zock PL, Taddei S, Deanfield JE, Luscher T, Green DJ, Ghiadoni L. Expert consensus and evidence-based recommendations for the assessment of flow-mediated dilation in humans. Eur. Heart J. 2019;40:2534-2547. doi: 10.1093/eurheartj/ehz350. PMID: 31211361.

21. Aroom KR, Harting MT, Cox CS, Radharkrishnan RS, Smith C, Gill BS. Bioimpedance Analysis: A Guide to Simple Design and Implementation. J. Surg. Res. 2009;153:23-30. doi: 10.1016/j.jss.2008.04.019. PMID: 18805550. PMCID: PMC3777733.

22. Pitella E, Piuzzi E, Rizzuto E, Pisa S, Del Prete Z. Metrological characterization of a combined bio-impedance plethysmograph and spectrometer. Measurement 2018;120:221-239. doi: 10.1016/j.measurement.2018.02.032.

23. Nebuya S, Mills GH, Milnes P, Brown BH. Indirect measurement of lung density and air volume from electrical impedance tomography (EIT) data. Physiol. Meas. 2011;32:1953-1967. doi: 10.1088/0967-3334/32/12/006. PMID: 22048128.

24. Vine SM, Painter PL, Kuskowski MA, Earthman CP. Bioimpedance spectroscopy for the estimation of fat-free mass in end-stage renal disease. E Spen Eur. E-J. Clin. Nutr. Metab. 2011;6:e1-e6. doi: 10.1016/j.eclnm.2010.12.003. PMID: 21552363. PMCID: PMC3086785.

25. Evgenidis SP, Karapantsios TD. Effect of bubble size on void fraction fluctuations in dispersed bubble flows. Int J. Multiph. Flow 2015;75:163-173. doi: 10.1016/j.ijmultiphaseflow.2015.05.013.

26. Evgenidis SP, Karapantsios TD. Gas–liquid flow of sub-millimeter bubbles at low void fractions: Experimental study of bubble size distribution and void fraction. Int. J. Heat Fluid Fl. 2018;71:353-365. doi: 10.1016/j.ijheatfluidflow.2018.04.011.

27. Evgenidis SP, Karapantsios TD. Gas-liquid flow of sub-millimeter bubbles at low void fractions: Void fraction prediction using drift-flux model. Exp. Therm. Fluid Sci. 2018;98:195-205. doi: 10.1016/j.expthermflusci.2018.05.018.

28. Evgenidis SP, Karapantsios TD. Pulsatile gas-liquid flow resembling Decompression Sickness: Computational Fluid Dynamics simulation and experimental validation. Int. Marit. Health. 2022;73(4):189-198. doi: 10.5603/IMH.2022.0033. PMED: 36583406.

29. Gkotsis PK, Evgenidis SP, Karapantsios TD. Influence of Newtonian and non-Newtonian fluid behavior on void fraction and bubble size for a gas-liquid flow of sub-millimeter bubbles at low void fractions. Exp. Therm. Fluid Sci. 2019;109:109912. doi: 10.1016/j.expthermflusci.2019.109912.

30. Gkotsis PK, Evgenidis SP, Karapantsios TD. Associating void fraction signals with bubble clusters features in co-current, upward gas-liquid flow of a non-Newtonian liquid. Int J. Multiph. Flow 2020;131:103297. doi: 10.1016/j.ijmultiphaseflow.2020.103297.

31. Balestra C, Theunissen S, Papadopoulou V, Le Mener C, Germonpré P, Guerrero F, Lafere P. Predive Whole-Body Vibration Better Reduces Decompression-Induced Vascular Gas Emboli than Oxygenation or a Combination of Both. Front. Physiol. 2016;7:586. doi: 10.3389/fphys.2016.00586. PMID: 27965591. PMCID: PMC5127795.

32. Germonpré P, Balestra C. Preconditioning to Reduce Decompression Stress in Scuba Divers. Aerosp. Med. Hum. Perf. 2017;88(2):114-120. doi: 10.3357/AMHP.4642.2017. PMID: 28095955.

33. Germonpré P, Papadopoulou V, Hemelryck W, Obeid G, Eckersley RJ, Tang M-X, Balestra C. The use of portable 2D echocardiography and "frame-based" bubble counting as a tool to evaluate diving decompression stress. Diving Hyperb. Med. 2014;44(1):5-13. PMID: 24687479.

34. Karapantsios T, Papara M. On the design of electrical conductance probes for foam drainage applications: Assessment of ring electrodes performance and bubble size effects on measurements. Colloids Surf. A Physicochem. Eng. Asp. 2008;323:139-148. doi: 10.1016/j.colsurfa.2007.10.003.

35. Devia F, Fossa M. Design and optimisation of impedance probes for void fraction measurements. Flow. Meas. Instrum. 2003;14: 139-149. doi: 10.1016/S0955-5986(03)00019-0.

36. Yang HC, Kim DK, Kim MH. Void fraction measurement using impedance method. Flow Meas. Instrum. 2003;14: 151-160. doi: https://doi.org/10.1016/S0955-5986(03)00020-7.

37. Grimnes S, Martinsen OG. Bioimpedance and Bioelectricity Basics, 2nd Edition, London (UK), Elsevier, 2008.

38. Golczewski T. Arterial blood flow waveform shapes – their original quantification and importance in chosen aspects of physiology and psychology: A review. Biocybern. Biomed. Eng. 2021;41:1418-1435. doi: 10.1016/j.bbe.2021.04.007.

39. Greenland S, Senn SJ, Rothman KJ, Carlin JB, Poole C, Goodman SN, Altman DG. Statistical tests, P values, confidence intervals, and power: a guide to misinterpetations. Eur. J. Epidemiol. 2016;31:337-350. doi: 10.1007/s10654-016-0149-3. PMID: 27209009. PMCID: PMC4877414.

40. Lee EC, Whitehead AL, Jacques RM, Julious SA. The statistical interpretation of pilot trials: should significance thresholds be reconsidered? BMC Medical Res. Methodol. 2014;14:41. doi: 10.1186/1471-2288-14-41.

41. Evgenidis SP, Chondrou A., Karapantsios TD. A new phantom that simulates electrically a human blood vessel surrounded by tissues: Development and validation against in-vivo measurements. Ann. Biomed. Eng. 2023;51(6):1284-1295. doi: 10.1007/s10439-022-03131-8.

42. Brebeck A-K, Deussen A, Range U, Balestra C, Cleveland S, Schipke JD. Beneficial effect of enriched air nitrox on bubble formation during scuba diving. An open-water study. J. Sports Sci. 2018;36(6):605-612. doi: 10.1080/02640414.2017.1326617.

43. Boussuges A, Retali G, Bodere-Melin M, Gardette B, Carturan D. Gender differences in circulating bubble production after SCUBA diving. Clin. Physiol. Funct. Imaging 2009;29(6):400-405. doi: 10.1111/j.1475-097X.2009.00884.x.

44. Kim D-J, Han J-W. Latent Class Analysis of Decompression Sickness Symptoms of Women Divers. Healthcare 2022;10(7):1246. doi: 10.3390/healthcare10071246.

45. Di Pasquale M. Sex Differences in Diving: Fact or Folklore. Curr. Sports Med. Rep. 2016;15(6):389-391. doi: 10.1249/JSR.0000000000000313.